Finite elements for vibration analysis of unsymmetric laminated composite plates

ARTICLE *in* MECHANICS OF ADVANCED MATERIALS AND STRUCTURES · JANUARY 1998

Impact Factor: 0.77 · DOI: 10.1080/10759419808945890

Mechanics of Advanced Materials and Structures
Publication details, including instructions for authors and subscription information:
http://www.informaworld.com/smpp/title~content=t713773278

FINITE ELEMENTS FOR VIBRATION ANALYSIS OF UNSYMMETRIC LAMINATED COMPOSITE PLATES

B. Bhattacharya [a]; A. V. Krishna Murty [a]; M. Seetharama Bhat [a]
[a] Department of Aerospace Engineering, Indian Institute of Science, Bangalore, India

Online Publication Date: 01 January 1998

To cite this Article Bhattacharya, B., Murty, A. V. Krishna and Bhat, M. Seetharama(1998)'FINITE ELEMENTS FOR VIBRATION ANALYSIS OF UNSYMMETRIC LAMINATED COMPOSITE PLATES',Mechanics of Advanced Materials and Structures,5:1,5 — 23
To link to this Article: DOI: 10.1080/10759419808945890
URL: http://dx.doi.org/10.1080/10759419808945890

FINITE ELEMENTS FOR VIBRATION ANALYSIS OF UNSYMMETRIC LAMINATED COMPOSITE PLATES

B. Bhattacharya, A. V. Krishna Murty, and M. Seetharama Bhat
Department of Aerospace Engineering, Indian Institute of Science, Bangalore, India

A 38-DOF (degrees-of-freedom), high precision triangular element is developed for vibration analysis of laminated composite panels with explicitly defined stiffness and mass matrices. A new, reduced-order, 18-DOF, high-precision element is formulated through condensation of the 38-DOF element; the order reduction is done at the element level instead of the conventional condensation at the postassembly global matrix level. Natural frequencies and mode shapes obtained using these two elements are compared with those available in the literature. Results indicate excellent performance of the condensed element. In view of the relatively lower DOF, the reduced element is believed to be attractive for evaluating dynamic response and vibration control analysis of unsymmetric laminates.

Structural designers prefer composite materials because of higher strength–weight ratios and more flexibility in tailoring required structural properties. The use of such materials to build lightweight structures, particularly for aerospace applications, often requires computationally economic algorithms to model their dynamic behavior.

The study of vibration of laminated composite plates and shells has received attention for over three decades. The reviews of Leissa [1], Reddy [2], and Kapania [3] cover the advances in this field extensively. The difficulties in obtaining closed-form solutions have led to the development of numerous approximate methods, of which the finite-element technique has been found to be the most powerful tool for the analysis of structures having complex shape and boundary constraints. Performance of high-precision finite elements is known to be generally better than that of elements based on conventional translational and rotational degrees of freedom, as the high-precision finite elements use higher-degree polynomial displacement functions, resulting in more accurate dynamic response. Shiau and Wu [4], for example, have developed a 72-degrees-of-freedom (DOF) triangular plate element considering the displacements and their higher-order derivatives as DOF. With such an element, it is possible to obtain precise solutions for natural frequencies and mode shapes, nearly as good as that of a three-dimensional elasticity model. However, in view of the large number of nodal degrees of freedom, such elements are not attractive for

Received 1 August 1996; accepted 1 April 1997.

This work has been partly supported by ARDB, Ministry of Defence, Government of India, under grant AERO/RD-134/100/10/94-95.

Address correspondence to Professor A. V. Krishna Murty, Department of Aerospace Engineering, Indian Institute of Science, Bangalore 560 012, India. E-mail: avk@aero.iisc.ernet.in

Mechanics of Composite Materials and Structures, 5:5–23, 1998

1075–9417/98 $12.00 + .00

vibration analysis, particularly when active control of the dynamic behavior is to be considered. As has been observed by Bhimraddy [5], composite plates may be analyzed fairly accurately using classical laminated plate theory (CLPT) over a wide range of thicknesses, and so high-precision elements based on CLPT, such as Cowper elements [6], may be attractive for laminate vibration analysis. However, to achieve faster and economic solution, complete elimination of expensive numerical integrations from the formulation of the element matrices and condensation of the element degrees of freedom are very desirable. The present article considers both of these aspects.

It is now well known that numerical integrations associated with element formulation may be eliminated using the SAN (symbolic-analytical-numerical) approach. One of the earliest references to this technique may be found in Pederson [7]. Using a symbolic manipulation language called PL/I-FORMAC, he obtained closed-form expressions for matrix multiplications, inversions, and numerical integrations needed to generate a linear-strain tetrahedron finite element. Subsequently, another software called REDUCE was used [8, 9] to compute closed-form stiffness matrices, and a shape optimization was carried out using mathematical programming. Using MATHEMATICA, Choi and Nomura [10] reported an extensive study of such technique for analyzing a rectangular body subjected to linear temperature distribution. These symbolic approaches have several advantages, such as automatic generation of the required polynomials, closed-form expressions for element matrices, and reduction of solution times.

Dynamic condensation procedures reduce the element DOF and the size of the eigenvalue problem, thereby reducing the computational effort. For many engineering problems, only the first few natural frequencies are of interest from the structural designer's point of view, as the probability of excitation of higher-order modes is very low. The DOF, having minor contribution to the total energy of the system at lower modes, can therefore be condensed [11]. Pas [12], perhaps the earliest, has proposed an iterative procedure in which the less important DOF are condensed, one by one, from the assembled matrix. A criterion for choosing the ignorable degrees of freedom using the ratios of the corresponding diagonal terms of the stiffness and mass matrices has been given by Hensell and Ong [13]. Thomas [14] has modified this criterion using an error norm in frequency estimation, considering the higher-order effects of the DOF to be condensed on the retained DOF. Unfortunately, this requires the solution of a nonlinear eigenvalue problem, which is difficult, particularly for a large assembled matrix.

In quest of an economic finite element for unsymmetric laminates, the present article has integrated the two aforementioned concepts. The numerical integration is replaced by closed-form analytic expressions. A 38-DOF triangular element, developed earlier by Jeychandra Bose and Kirkhope [15, 16] for static analysis, is adopted here to study the vibration of unsymmetric composite plates. MATHEMATICA is used to derive the elements of mass and stiffness matrices in closed form for the first time. A two-stage static and dynamic condensation of these matrices is carried out at the element level itself to generate a new, 18-DOF triangular element. Both 38- and 18-DOF elements are used to obtain results for unsymmetric rectangular and skewed composite plates and also plates having cutouts. Comparison of the results with some of those available in the literature brings out the performance of these elements.

THE FINITE-ELEMENT FORMULATION

In [6], Cowper developed a triangular thin-plate element, with the transverse deflections and their first- and second-order derivatives as DOF, and the displacement function

in the form of a constrained quintic polynomial. In this element, the interelement continuity of normal slope is satisfied, which is a cubic function of the edgewise coordinate. This element has excellent convergence properties and is usually referred as a high-precision element (HPE). In the present element, in addition to the transverse DOF, the in-plane displacements and their first-order derivatives are also included as DOF. The in-plane DOF are added in order to make the element applicable to unsymmetric composite laminates. Two centroidal in-plane DOF (u_c and v_c) are also considered to facilitate the use of a complete cubic polynomial for in-plane displacements. This element has 38 DOF and will be referred to henceforth as HPE-38. The element configuration is shown in Figure 1.

In each element, three field displacements, u, v (in-plane components), and w (transverse component) along the x, y, and z directions are considered. Nodal DOF chosen are grouped into three vectors as

$$\{\delta\}^T = \{\{U\}^T, \{V\}^T, \{W\}^T\} \tag{1}$$

where

$$\{U\}^T = \{u_1, u_{\xi 1}, u_{\eta 1}, u_2, \ldots, u_{\eta 3}, u_c\}_{10\times 1} \tag{2}$$

$$\{V\}^T = \{v_1, v_{\xi 1}, v_{\eta 1}, v_2, \ldots, v_{\eta 3}, v_c\}_{10\times 1} \tag{3}$$

$$\{W\}^T = \{w_1, w_{\xi 1}, w_{\eta 1}, w_{\xi\xi 1}, w_{\xi\eta 1}, w_{\eta\eta 1}, w_2, \ldots, w_{\eta\eta 3},\}_{18\times 1} \tag{4}$$

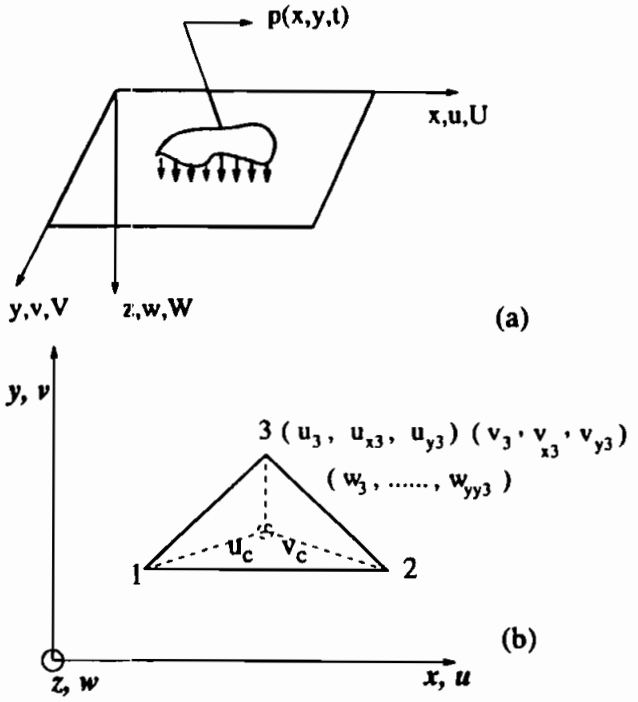

Figure 1. Element configuration.

u_{xi}, w_{xi}, etc., are the first-order derivatives with respect to x at node i ($i = 1, 2, 3$). Similarly, w_{xxi}, etc., are the second-order derivatives; u_c, v_c denote the displacements along x and y directions at the centroid of the element. The in-plane displacement functions are assumed to be complete cubic polynomials:

$$u(\xi, \eta) = \{\Lambda_1\}^T \{\mathbf{C}\} \tag{5}$$

where

$$\{\Lambda_1\}^T = \{1, \xi, \eta, \ldots, \eta^3\}$$

and

$$\{\mathbf{C}\}^T = \{C_1, \ldots, C_{10}\}$$

For the transverse displacement function,

$$w(\xi, \eta) = \{\Lambda_2\}^T \{\overline{\mathbf{C}}\} \tag{6}$$

where

$$\{\Lambda_2\}^T = \{1, \xi, \eta, \ldots, \eta^4, \xi^5, \xi^3\eta^2, \xi^2\eta^3, \xi\eta^4, \eta^5\}$$
$$\{\overline{\mathbf{C}}\}^T = \{C_{21}, \ldots, C_{40}\}$$

It may be noted that in $\{\Lambda_2\}$, the $\xi^4\eta$ term is dropped in order to provide the cubic variation of the normal slope along the edge $\eta = 0$. Using Eqs. (1)–(6), the displacement field can be expressed in terms of nodal displacements as

$$\begin{aligned} u(\xi, \eta) &= [\mathbf{N}] \{\mathbf{U}\} \\ v(\xi, \eta) &= [\mathbf{N}] \{\mathbf{V}\} \\ w(\xi, \eta) &= [\overline{\mathbf{N}}] \{\mathbf{W}\} \end{aligned} \tag{7}$$

where

$$[\mathbf{N}] = \{\Lambda_1\}^T [\mathbf{T}_1]^{-1}$$

and

$$[\overline{\mathbf{N}}] = \{\Lambda_2\}^T [\mathbf{T}_2]^{-1}$$

where $\mathbf{T}_1^{-1}$ can be obtained directly by using Eqs. (2) and (5); $\mathbf{T}_2^{-1}$ is to be evaluated using Eqs. (4) and (6) and the constraint conditions to achieve the continuity of the normal slope across the element boundaries [6]. Using MATHEMATICA, [N] and [$\overline{\mathbf{N}}$]

are evaluated explicitly. Closed-form expressions of these two matrices are already reported in [15] and [16].

Stiffness Matrix

Following Kirchhoff-Love's assumptions, the expressions for strains are given by

$$\begin{aligned} \epsilon_x &= u_{,x} - zw_{,xx} \\ \epsilon_y &= v_{,y} - zw_{,yy} \\ \gamma_{xy} &= u_{,y} + v_{,x} - 2\,zw_{,xy} \end{aligned} \tag{8}$$

or

$$\{\epsilon\} = \{\epsilon^0\} + z\,\{\chi\}$$

Assuming each lamina to be orthotopic, the constitutive relations can be written as

$$\{\sigma\} = [\overline{\mathbf{Q}}]\,\{\epsilon\}$$

where

$$\{\sigma\}^T = \{\sigma_x, \sigma_y, \sigma_{xy}\}$$
$$\{\epsilon\}^T = \{\epsilon_x, \epsilon_y, \gamma_{xy}\}$$

and the reduced stiffness matrix $\overline{\mathbf{Q}}$ can be computed from the material properties, fiber orientation angles, etc. [18]. The expression for strain energy, $\mathcal{U}$, may be written as

$$\mathcal{U} = \frac{1}{2}\int_A [\{\epsilon^0\}^T [\mathbf{A}]\,\{\epsilon^0\} + \{\epsilon^0\}^T [\mathbf{B}]\,\{\mathbf{X}\} + \{\mathbf{X}\}^T [\mathbf{B}]\,\{\epsilon^0\} + \{\chi\}^T [\mathbf{D}]\,\{\chi\}]\,dA \tag{9}$$

where

$$(A_{ij}, B_{ij}, D_{ij}) = \sum_{k=1}^{n} \int_{h_k}^{h^{k+1}} (\overline{Q}_{ij})_k\,(1, z, z^2)\,dz$$

n = total number of layers and h_k = distance of the kth layer of lamina from the origin, and [**B**] is the coupling matrix, which is zero for symmetric laminates and is nonzero for unsymmetric laminates.

The strain and curvature vectors can be expressed in terms of area coordinates, and Eq. (9) can be rearranged as

$$\mathcal{U} = \frac{1}{2}\int_0^1 \int_0^{1-\xi} [\{\alpha\}^T [\bar{\mathbf{A}}] \{\alpha\} + \{\alpha\}^T [\bar{\mathbf{B}}] \{\beta\} + \{\beta\}^T [\bar{\mathbf{B}}] \{\alpha\} + \{\beta\}^T [\bar{\mathbf{D}}] \{\beta\}] \, d\xi \, d\eta \tag{10}$$

with

$$\begin{aligned} \{\alpha\}^T &= [u_\xi, u_\eta, v_\xi, v_\eta] \\ \{\beta\}^T &= -[w_{\xi\xi}, w_{\eta\eta}, w_{\xi\eta}] \end{aligned} \tag{11}$$

and

$$[\bar{\mathbf{A}}] = \frac{1}{2\Delta} [\mathbf{P}]^T [\mathbf{A}][\mathbf{P}]$$

$$[\bar{\mathbf{B}}] = \frac{1}{2\Delta^2} [\mathbf{P}]^T [\mathbf{B}][\mathbf{Q}]$$

$$[\bar{\mathbf{D}}] = \frac{1}{2\Delta^3} [\mathbf{Q}]^T [\mathbf{D}][\mathbf{Q}]$$

where

$$[\mathbf{P}] = \begin{bmatrix} b_1 & b_2 & 0 & 0 \\ 0 & 0 & c_1 & c_2 \\ c_1 & c_2 & b_1 & b_2 \end{bmatrix}$$

$$[\mathbf{Q}] = \begin{bmatrix} b_1^2 & b_2^2 & 2b_1b_2 \\ c_1^2 & c_2^2 & 2c_1c_2 \\ 2b_1c_1 & 2b_2c_2 & 2(b_1c_2 + b_2c_1) \end{bmatrix}$$

Using Eqs. (1)–(6); α and β can be expressed in terms of nodal DOF and the element stiffness matrix can be identified from the strain energy expression in the form

$$\mathcal{U} = \frac{1}{2} \begin{Bmatrix} \mathbf{U}^T \\ \mathbf{V}^T \\ \mathbf{W}^T \end{Bmatrix} [\mathbf{K}] \begin{Bmatrix} \mathbf{U} \\ \mathbf{V} \\ \mathbf{W} \end{Bmatrix}$$

where [K] is the stiffness matrix, which is a function of **N**, $\bar{\mathbf{N}}$, **A**, **B**, and **D**. In the present study, elements of [K] are obtained in explicit form using MATHEMATICA and are given in the authors' report [19]. The elimination of numerical integration alleviates the problem of choosing proper order of integration and improves the computation time.

Mass Matrix

The mass matrix may be identified from the expression for kinetic energy $\mathcal{T}$:

$$\mathcal{T} = \frac{1}{2}\int_v \rho[\dot{u}^T \dot{u} + \dot{v}^T\dot{v} + \rho\dot{w}^T\dot{w}]\, dV$$

or

$$\mathcal{T} = \frac{1}{2}\int_v \rho[\dot{\mathbf{U}}^T \mathbf{N}^T\mathbf{N}\dot{\mathbf{U}} + \dot{\mathbf{V}}^T\mathbf{N}^T\mathbf{N}\dot{\mathbf{V}} + \dot{\mathbf{W}}^T\overline{\mathbf{N}}^T\overline{\mathbf{N}}\dot{\mathbf{W}}]\, dV \tag{12}$$

as

$$\mathbf{M} = \sum_{k=1}^{n} \Delta t_k \rho_k \iint [\mathbf{N}_s^T\, \mathbf{N}_s]\, dx\, dy \tag{13}$$

where Δt_k = thickness of the kth layer, ρ_k = density per unit area of the kth layer, and

$$\mathbf{N}_s = \begin{bmatrix} \mathbf{N} & 0 & 0 \\ 0 & \mathbf{N} & 0 \\ 0 & 0 & \overline{\mathbf{N}} \end{bmatrix}$$

On transformation to area coordinates, Eq. (13) becomes

$$\mathbf{M} = \psi \int_0^1 \int_0^{1-\xi} [\mathbf{N}_s^T\mathbf{N}_s]\, d\xi\, d\eta$$

$$\psi = \sum_{k=1}^{n} \Delta t_k \rho_k 2\Delta$$

Assuming the thickness and density to be uniform within each element, and noting that the expression for $\mathbf{N}_s$ contains $\mathbf{\Lambda}_1$ and $\mathbf{\Lambda}_2$ only, the following two integrals are necessary to evaluate $\mathbf{M}$ in closed form:

$$\mathbf{P}_1 = \int_0^1 \int_0^{1-\xi} [\mathbf{\Lambda}_1\mathbf{\Lambda}_1^T]\, d\xi\, d\eta \tag{14}$$

$$\mathbf{P}_2 = \int_0^1 \int_0^{1-\xi} [\mathbf{\Lambda}_2\mathbf{\Lambda}_2^T]\, d\xi\, d\eta \tag{15}$$

Recognizing that Λ_1 is a subset of Λ_2, Λ_2^T is partitioned for convenience as $[\Lambda_1^T|\overline{\Lambda}_1^T]$, resulting in

$$\Lambda_2\Lambda_2^T = \begin{bmatrix} \Lambda_1\Lambda_1^T & \Lambda_1\overline{\Lambda}_1^T \\ \overline{\Lambda}_1\Lambda_1^T & \overline{\Lambda}_1\overline{\Lambda}_1^T \end{bmatrix}$$

thereby $\mathbf{P}_2$ may be written as

$$\mathbf{P}_2 = \begin{bmatrix} \mathbf{P}_1 & \mathbf{PM}_{12} \\ \mathbf{PM}_{21} & \mathbf{PM}_{22} \end{bmatrix}$$

and $\mathbf{PM}_{12} = \mathbf{PM}_{21}^T$. Matrices $\mathbf{P}_1$, $\mathbf{PM}_{12}$, and $\mathbf{PM}_{22}$ are evaluated by MATHEMATICA. After obtaining the matrices $\mathbf{PM}_1$ and $\mathbf{P}_2$ the mass matrix elements are formed using Eqs. (7) and (13). Elements of the mass matrix $\mathbf{M}$, in closed form, are somewhat lengthy and are given in [19].

DYNAMIC ANALYSIS

The dynamic equations of equilibrium are formulated in the standard way as

$$[\mathbf{M}_g]\{\ddot{\delta}\} + [\mathbf{K}_g]\{\delta\} = \mathbf{0} \tag{16}$$

where $\mathbf{M}_g$ and $\mathbf{K}_g$ are global matrices assembled from element matrices. Assuming a general solution of the form $\delta = \delta_a e_{i\omega t}$, the eigenvalue problem is constructed as

$$[\mathbf{K}_g]\{\delta_a\} = \lambda[\mathbf{M}_g]\{\delta_a\}$$

where $\lambda = \omega^2$.

The HPE-38 has 12 degrees of freedom per node; as a result, the size of the eigenvalue problem is usually much larger than the number of frequencies required. A good amount of computational time can be saved if a solution scheme is adopted that is capable of finding only the required number of eigenvalues instead of solving for all eigenvalues. The subspace iteration method, used in this article, is one of the best techniques for this purpose. Starting with a subspace of assumed vectors with dimension equal to the number of required eigenvalues, an iterative procedure is adopted to obtain the desired frequencies and mode shapes. This solution technique requires approximately $nm^2 + nm(4 + 4r) + 5nr + 20nq(2m + q + 3/2)$ numbers of operations, where n denotes the size of the matrix involved, m is the half-bandwidth, r is the number of eigenvalues required, and $q = \min(2r, r + 8)$ [20]. For eigenvalue problems having total DOF more than 1000, solution is difficult even with such routines, and it is expedient to explore possibilities for reduction of DOF.

Condensation of some of the DOF is a widely accepted way of reducing size of an eigenvalue problem. Usually the method is adopted after assembling the element matrices into global $\mathbf{M}_g$ and $\mathbf{K}_g$. Here, an alternative semianalytic condensation scheme is proposed that can be applied directly at the element level. It is found that the two centroidal DOF u_c and v_c of each element are isolated from the other elements, unlike the DOF at the

vertices. Hence, in the first-stage these two in-plane DOF of each element are condensed statically for convenience. Thus, the original eigenvalue problem $\mathbf{K}x = \lambda \mathbf{M}x$ is modified as

$$\overline{\mathbf{K}}\boldsymbol{\delta}_1 = \lambda \overline{\mathbf{M}}\boldsymbol{\delta}_1 \tag{17}$$

where $\boldsymbol{\delta}_1$ are the set of DOF to be retained and $\boldsymbol{\delta}_2$ are the DOF to be condensed. Then the modified stiffness and mass matrices of the reduced eigenvalue problem can be written as

$$\begin{aligned} \overline{\mathbf{K}} &= \mathbf{K}_{11} - \mathbf{K}_{12}\,\mathbf{K}_{22}^{-1}\mathbf{K}_{21} \\ \overline{\mathbf{M}} &= \mathbf{M}_{11} \end{aligned} \tag{18}$$

In the second stage of condensation, the inertia forces corresponding to the slave DOF (DOF to be condensed) are not negligible in comparison to the master DOF (DOF to be retained). Hence, assuming that the slave DOF are negligible excited, dynamic condensation of stiffness and mass matrices are carried out. In this article, the dynamic condensation technique is applied at the element level. The successful use of such a technique for condensing DOF in a simply supported Timoshenko beam is reported in the literature [14]. To eliminate the slave DOF at the element level, a suitable relationship of the slave DOF with the masters is essential. Here we create such a relationship by assuming dynamic equilibrium at each element. It must be remembered that this is only approximate and approaches the true situation only when the boundaries are not constrained. The steps of dynamic condensation are as follows.

The slave DOF are identified comparing the constrained eigenfrequency ratio expressions of all the 36 DOF retained after the first stage of condensation. Accordingly, only 18 DOF (w_i, $w_{,xi}$, $w_{,yi}$, $w_{,xxi}$, $w_{,xyi}$, $w_{,yyi}$, $i = 1, \ldots, 3$) are selected as master DOF, and a new element RHPE-18 is formed. It may be noted that the truncation from 36 DOF to 18 DOF results in a Cowper element, whereas the condensation brings out a new element with modified stiffness and mass matrices.

As $(\mathbf{K} - \lambda\mathbf{M})\boldsymbol{\delta} = 0$ for each element, partitioning the vector $\boldsymbol{\delta}$ into master and slave DOF based on the previous step results in

$$\left(\begin{bmatrix} \mathbf{K}_{mm} & \mathbf{K}_{ms} \\ \mathbf{K}_{sm} & \mathbf{K}_{ss} \end{bmatrix} - \lambda \begin{bmatrix} \mathbf{M}_{mm} & \mathbf{M}_{ms} \\ \mathbf{M}_{sm} & \mathbf{M}_{ss} \end{bmatrix} \right) \begin{Bmatrix} \boldsymbol{\delta}_m \\ \boldsymbol{\delta}_s \end{Bmatrix} = \{\mathbf{0}\} \tag{19}$$

Assuming that at the lower frequencies of interest there will be no excitation of the slave DOF, they can be eliminated using

$$\boldsymbol{\delta}_s = -(\mathbf{K}_{ss} - \lambda\mathbf{M}_{ss})^{-1}(\mathbf{K}_{sm} - \lambda\mathbf{M}_{sm})\boldsymbol{\delta}_m \tag{20}$$

However, a computationally feasible way is found out to eliminate $\boldsymbol{\delta}_s$ and obtain a modified eigenvalue problem.

For this purpose, consider the auxiliary eigenvalue problem pertaining to $\boldsymbol{\delta}_s$ constraining the motion of masters ($\boldsymbol{\delta}_m = \mathbf{0}$), which is, in this case, the 18 DOF consisting of all in-plane DOF:

$$(\mathbf{K}_{ss} - \lambda_s \mathbf{M}_{ss})\boldsymbol{\delta}_s = \mathbf{0}$$

or, after modal transformation,

$$(\mathbf{K}_{ss} - \boldsymbol{\Lambda}_s \mathbf{M}_{ss})\tilde{\boldsymbol{\Phi}} = \mathbf{0} \tag{21}$$

where $\boldsymbol{\Lambda}_s$ is a diagonal matrix with eigenvalues λ_{si} and $\tilde{\boldsymbol{\Phi}}$ is a square matrix with eigenvectors $\boldsymbol{\delta}_{si}$. If $\mathbf{W}$ is a normalizing vector required for mass orthonormalization, then

$$\begin{aligned} \boldsymbol{\delta}_s &= \boldsymbol{\Phi}\mathbf{W} \\ \boldsymbol{\Phi}^T \mathbf{M}_{ss} \boldsymbol{\Phi} &= \mathbf{I} \\ \boldsymbol{\Phi}^T \mathbf{K}_{ss} \boldsymbol{\Phi} &= \boldsymbol{\Lambda}_s \end{aligned} \tag{22}$$

Substituting Eq. (22) into Eq. (20), $\boldsymbol{\delta}_s$ can be re-formed as

$$\boldsymbol{\delta}_s = -\boldsymbol{\Phi}\boldsymbol{\Lambda}_s^{-1}(\mathbf{I} - \lambda\boldsymbol{\Lambda}_s^{-1})^{-1}\boldsymbol{\Phi}^T(\mathbf{K}_{sm} - \lambda\mathbf{M}_{sm})\boldsymbol{\delta}_m$$

When $\lambda < \lambda_{s(\min)}$ (which provides a criterion for selection of master DOF), by denoting $\lambda\boldsymbol{\Lambda}_s^{-1} = \boldsymbol{\gamma}$ ($\boldsymbol{\gamma}$ is a diagonal matrix having $\gamma_{ii} < 1$, $\boldsymbol{\gamma}^2 = \boldsymbol{\gamma}\boldsymbol{\gamma}$, $\boldsymbol{\gamma}^3 = \boldsymbol{\gamma}\boldsymbol{\gamma}\boldsymbol{\gamma}$, etc.), one gets

$$(\mathbf{I} - \lambda\boldsymbol{\Lambda}_s^{-1})^{-1} = (\mathbf{I} - \boldsymbol{\gamma})^{-1} = \mathbf{I} + \boldsymbol{\gamma} + \boldsymbol{\gamma}^2 + \cdots$$

Hence,

$$\begin{aligned} \boldsymbol{\delta}_s &= -\boldsymbol{\Phi}\boldsymbol{\Lambda}_s^{-1}(\mathbf{I} + \boldsymbol{\gamma} + \boldsymbol{\gamma}^2 + \cdots)\boldsymbol{\Phi}^T(\mathbf{K}_{sm} - \lambda\mathbf{M}_{sm})\boldsymbol{\delta}_m \\ &= \boldsymbol{\Phi}[-\boldsymbol{\Lambda}_s^{-1}\boldsymbol{\Phi}^T(\mathbf{K}_{sm} - \lambda\mathbf{M}_{sm}) - \boldsymbol{\Lambda}_s^{-1}\boldsymbol{\gamma}\boldsymbol{\Phi}^T(\mathbf{K}_{sm} - \boldsymbol{\gamma}\mathbf{M}_{sm}) \cdots]\boldsymbol{\delta}_m \end{aligned}$$

Defining $\mathbf{H} = -\boldsymbol{\Lambda}_s^{-1}\boldsymbol{\Phi}^T\mathbf{K}_{sm}$ and $\mathbf{T} = \mathbf{H} + \boldsymbol{\Phi}^T\mathbf{M}_{sm}$, we get a new expression for $\boldsymbol{\delta}_s$:

$$\boldsymbol{\delta}_s = \boldsymbol{\Phi}[\mathbf{H} + \boldsymbol{\gamma}(\mathbf{I} + \boldsymbol{\gamma} + \boldsymbol{\gamma}^2 + \cdots)\mathbf{T}]\boldsymbol{\delta}_m \tag{23}$$

Substituting Eq. (23) into Eq. (19) yields

$$\begin{aligned} [\mathbf{K}_{mm} + \mathbf{K}_{ms}\boldsymbol{\Phi}\mathbf{H} - \boldsymbol{\gamma}\boldsymbol{\Lambda}_s(\mathbf{M}_{mm} + \mathbf{M}_{ms}\boldsymbol{\Phi}\mathbf{H}) + \mathbf{K}_{ms}\boldsymbol{\Phi}\boldsymbol{\gamma}\mathbf{T} \\ - \boldsymbol{\gamma}\boldsymbol{\Lambda}_s\mathbf{M}_{ms}\boldsymbol{\Phi}\boldsymbol{\gamma}\mathbf{T} + \mathbf{K}_{ms}\boldsymbol{\Phi}\boldsymbol{\gamma}^2\mathbf{T} + \mathbf{O}(\boldsymbol{\gamma}^3)]\boldsymbol{\delta}_m = \mathbf{0} \end{aligned}$$

Consideration of only the first order of $\boldsymbol{\gamma}$ is generally inadequate, as it introduces significant computational error [14]. Hence, the second-order effect of $\boldsymbol{\gamma}$ is considered here. Noting that $\boldsymbol{\Phi}\boldsymbol{\Lambda}_s^{-1}\boldsymbol{\Phi}^T = \mathbf{K}_{ss}^{-1}$, the eigenvalue problem can be further simplified to

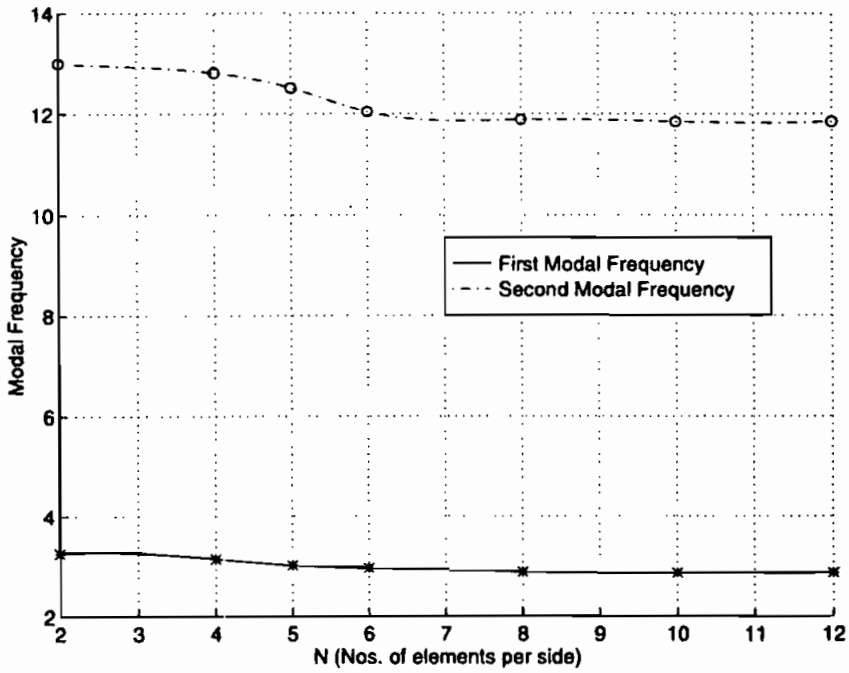

Figure 2. Convergence in frequency estimation by RHPE-18 corresponding to first and second modal frequencies.

$$(\mathbf{K}^R - \lambda\mathbf{M}^R - \lambda\delta\mathbf{M})\boldsymbol{\delta}_m = \mathbf{0} \tag{24}$$

where

$$\mathbf{K}^R = \mathbf{K}_{mm} - \mathbf{K}_{ms}\mathbf{K}_{ss}^{-1}\mathbf{K}_{sm}$$

$$\mathbf{M}^R = \mathbf{M}_{mm} + \mathbf{K}_{ms}\mathbf{K}_{ss}^{-1}\mathbf{M}_{ss}\mathbf{K}_{ss}^{-1}\mathbf{K}_{sm} - \mathbf{M}_{ms}\mathbf{K}_{ss}^{-1}\mathbf{K}_{sm} - \mathbf{K}_{ms}\mathbf{K}_{ss}^{-1}\mathbf{M}_{sm}$$

and

$$\delta\mathbf{M} = \mathbf{M}_{ms}\boldsymbol{\Phi}\boldsymbol{\gamma}\mathbf{T} - \mathbf{K}_{ms}\boldsymbol{\Phi}\boldsymbol{\Lambda}_s^{-1}\boldsymbol{\gamma}$$

$$\mathbf{T} = \mathbf{T}^T\boldsymbol{\gamma}\boldsymbol{\Lambda}_s^{-1}\mathbf{T}$$

Thus, in this step the following computations are to be made:

1. Numerical computation of $\boldsymbol{\Lambda}_s$ and $\mathbf{W}$ solving an 18×18 eigenvalue problem for each element
2. Computation of $\mathbb{H}$, $\mathbf{T}$, and $\delta\mathbf{M}$ based on $\boldsymbol{\Lambda}_s$ and $\mathbf{W}$
3. Computation of $\mathbb{K}^R$ and $\mathbf{M}^R$ for each element semianalytically, thus constituting a new 18-DOF element from the old element
4. Finally, solution of an eigenvalue problem using the Wittrick and Williams algorithm [23]

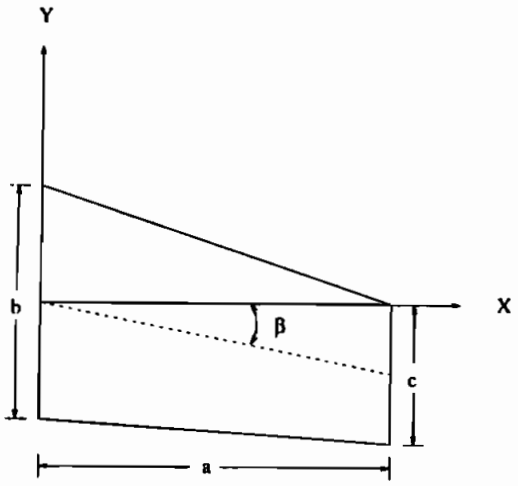

Figure 3. A typical swept plate.

Computer programs are written in FORTRAN in which closed-form expressions are directly used wherever possible with the help of MATHEMATICA.

RESULTS AND DISCUSSION

HPE-38 is a well-established element for static analysis. In dynamic analysis, too, it is known to converge well. The reduced-order RHPE-18, however, is a new derivative of the high-precision element. Figure 2 shows the convergence trend of RHPE-18 corresponding to the first and second modal frequencies of a cantilever plate. The results indicate that the frequency by RHPE-18 converges well with mesh refinement.

In the following discussion the performance of HPE-38 and RHPE-18 will be compared with the other results. First, a symmetric layup is considered in order to bring out the performance of the present elements in comparison with the results available in the literature. Typical problems of free vibration of unsymmetric laminates having different boundary conditions, and weak or strong orthotropic properties, are chosen subsequently for performance evaluation of HPE-38. Finally, the elements themselves are compared with respect to their performance in estimating the modal frequencies.

Cantilever Swept Composite Plate

The geometry of the plate is shown in Figure 3 and the finite-element mesh in Figure 4. The material properties of the composite laminate are considered the same as

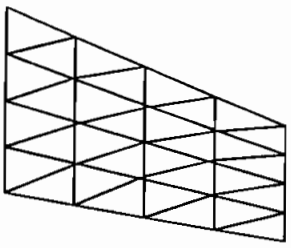

Figure 4. Finite-element mesh for swept plate.

Table 1. Comparison of nondimensional frequency parameter $\Omega = (\omega a^2/h)\sqrt{\rho/E_2}$ ($\beta = 30°$, $a = 14''$, $b = 6''$, $c = 3''$, taper ratio = 0.5, $S = 100$)

Laminate layup	Mode no.	Lee[a]	Lee[b]	HPE-38	RHPE-18
$[0_2/0]_s$	1	2.09	2.07	2.07	2.07
	2	10.08	10.13	10.06	10.06
	3	12.45	12.21	12.24	12.24
$[15_2/0]_s$	1	1.99	1.90	1.90	1.90
	2	9.34	9.24	9.22	9.22
	3	13.93	13.86	13.88	13.88
$[30_2/0]_s$	1	1.64	1.57	1.57	1.57
	2	8.41	8.25	8.27	8.27
	3	14.51	14.72	14.75	14.76
$[45_2/0]_s$	1	1.30	1.30	1.30	1.30
	2	7.34	7.20	7.24	7.24
	3	14.00	14.43	14.36	14.36
$[60_2/0]_s$	1	1.16	1.16	1.16	1.16
	2	6.59	6.44	6.46	6.46
	3	12.52	13.07	12.98	12.99
$[90_2/0]_s$	1	1.07	1.01	1.01	1.01
	2	5.90	5.76	5.81	5.81
	3	10.28	10.56	10.58	10.61

[a] Four-noded element.
[b] Eight-noded element.

in [21]. The length-to-thickness ratio S for the plate is 100. A symmetric ply sequence $[\theta_2/0]_s$ is chosen for numerical study. The number of active DOF considered is 185 for the HPE-38 element and 95 for the RHPE-18. The frequencies obtained from the (4 × 4) mesh agree well with Lee's results using four- and eight-noded rectangular elements (Table 1). Mode shapes are presented in Figure 5. Results of Lee [21] and the present elements are so close that they are shown by the same nodal line in these figures.

Anisotropic Square Plate

Next, the vibration of unsymmetric cross- and angle-ply laminates with fixed-fixed boundary condition has been considered. In view of the asymmetry, the B matrix is nonzero here. As the in-plane vibration is coupled with transverse motion, this example is useful to evaluate the effect of condensing in-plane DOF. Results corresponding to $S = 50$ and 100 with the material properties $E_1/E_2 = 40$, $G_{12}/E_2 = 0.6$, and $\nu_{12} = 0.25$ are compared with those of Reddy [24] and Shiau [4] (Table 2). Excellent performance of RHPE-18 may be noted. In view of the large reduction in DOF, without loss of much accuracy (0.01% relative error with RHPE-18), reduced elements may be considered attractive for dynamic analysis. Results for five sets of boundary conditions, *C–C–C–C*, *C–C–F–F*, *C–F–C–F*, *C–C–S–S*, and *C–S–C–S*, given in Table 3, shows that the reduced element predicts frequencies fairly accurately for all the cases.

Composite Plate with Rectangular Cutout

The accuracy of frequency estimation by the high-precision elements in the presence of a cutout is studied next. The free-vibration problem of a simply supported graphite-

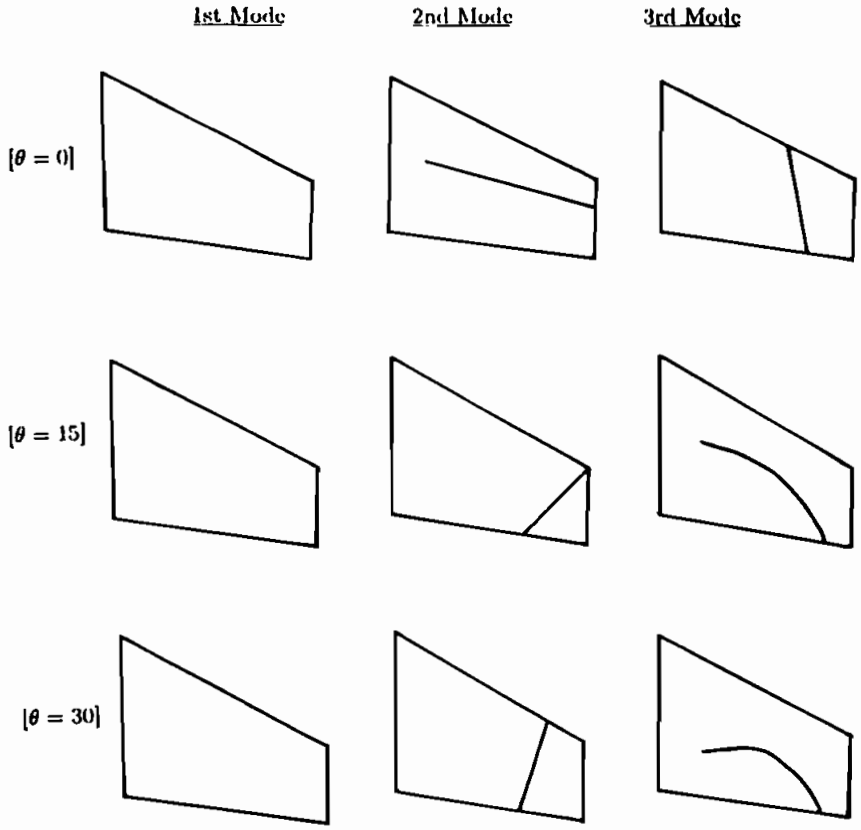

Figure 5. Mode shapes of swept composite plate; ply layup $[\theta_2/0]$; swept angle $\beta = 30°$.

epoxy square plate with a rectangular cutout at its center is considered. The orthotropic material properties are $E_x/E_y = 40$, $G_{xy}/E_y = 0.5$, and $\nu_{xy} = 0.25$. The plate geometry and the finite-element subdivision are shown in Figures 6 and 7, respectively. Variation of the nondimensional frequency parameter Ω with d/a for different sizes of cutouts is shown in Figures 8 and 9. For orthotropic plates, the results obtained by Lee et al. [22] through Ritz analysis are also plotted for comparison in Figure 7. In Figure 9 the performance of RHPE-18 is compared with HPE-38 for unsymmetric (0/90) laminates. The performance

Table 2. Fundamental frequencies (in Hz) of different square laminates

Laminate	S	Ref. [24]	HPE-38	RHPE-18
(0/90)	50	11.302	11.302	11.315
	100	11.306	11.306	11.309
(45/−45)	50	14.629	14.630	14.641
	100	14.635	14.634	14.639
$(\pm 45)_4$	50	25.257	25.257	25.272
	100	25.264	25.264	25.278

Table 3. Modal frequency estimation by HPE-38 and RHPE-18 corresponding to different boundary conditions

Boundary condition	Mode I (rad/s)		Mode II (rad/s)		Mode III (rad/s)	
	HPE-38	RHPE-18	HPE-38	RHPE-18	HPE-38	RHPE-18
C–C–C–C	18.20	18.24	29.08	29.18	55.34	55.92
C–C–F–F	10.95	10.97	27.37	27.41	46.27	46.42
C–F–C–F	10.22	10.28	26.16	26.26	45.33	45.50
C–C–S–S	13.52	13.61	26.14	26.21	48.18	48.33
C–S–C–S	14.85	14.98	24.34	24.39	47.18	47.40

of RHPE-18 is excellent for all combinations of *d/a* and *d/c*. The frequency parameters obtained using RHPE-18 for unsymmetric laminates for the first five modes are compared with results obtained using HPE-38 in Table 4 for various sizes of cutouts. Table 5 provides the corresponding modal vector data for the first two modes. The difference in nodal deflections, corresponding to the mode shapes, obtained using HPE-38 and RHPE-18 are very small.

Performance Comparison of HPE-38 and RHPE-18

Finally, the performance of HPE-38 and its derivative RHPE-18 are compared for a cantilever triangular plate. Fundamental frequency estimated by HPE-38 with a coarser

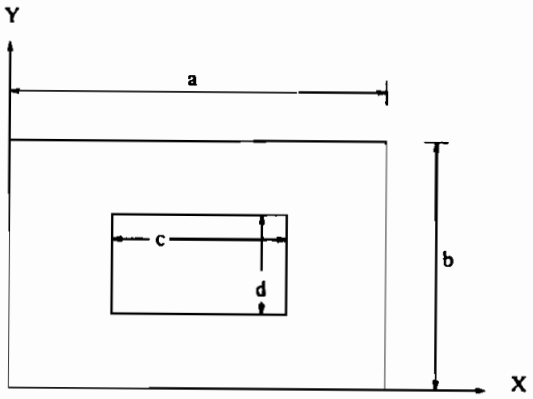

Figure 6. Simply supported rectangular plate with cutout.

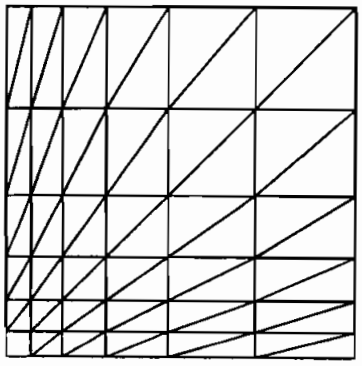

Figure 7. Typical finite element mesh for quarter-plate of rectangular cutout.

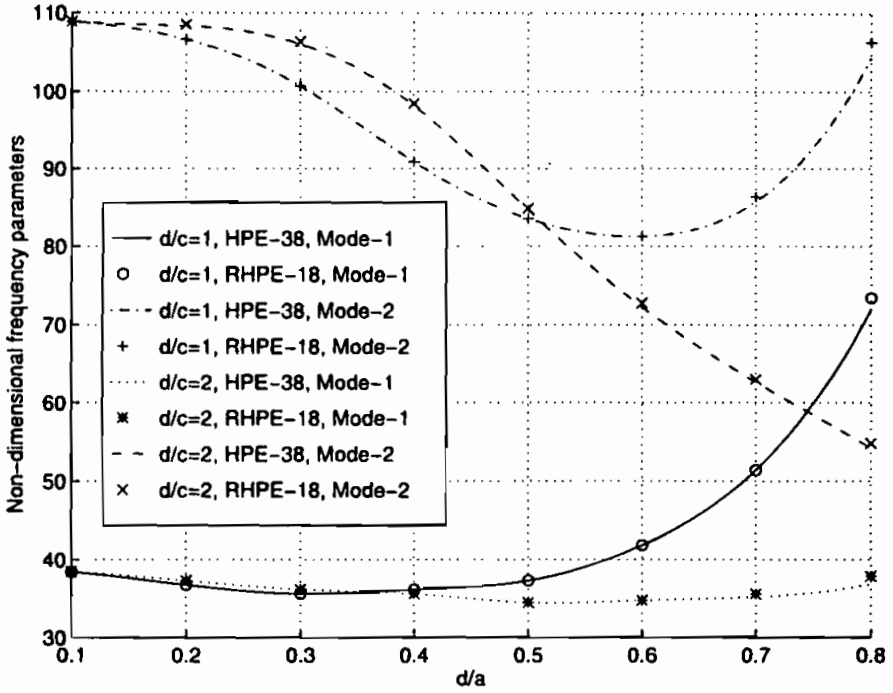

Figure 8. Fundamental frequency parameters for orthotropic square plate with a rectangular cutout.

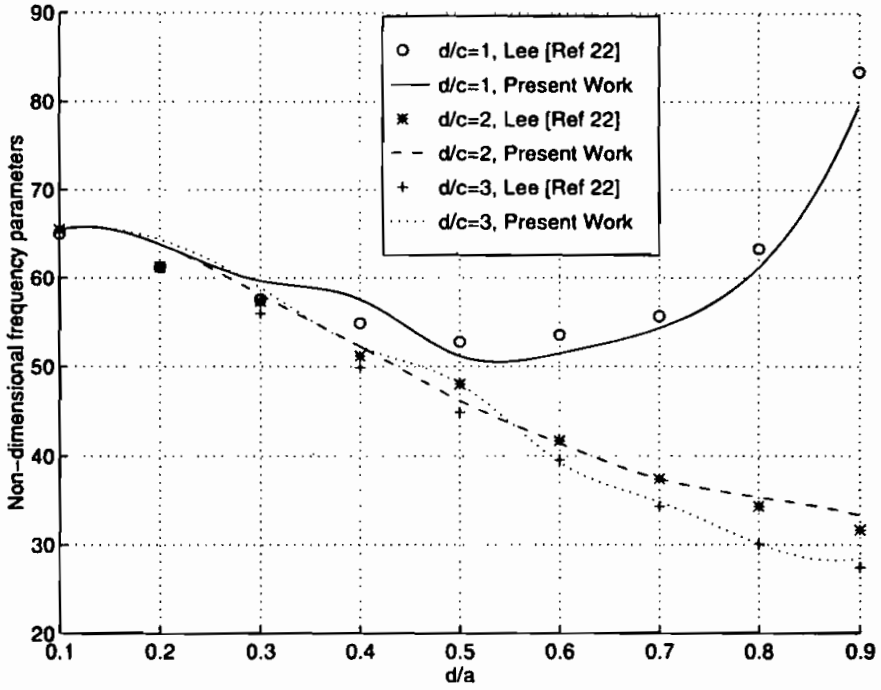

Figure 9. Frequency parameters for unsymmetric laminate with cutout.

Table 4. Nondimensional frequency parameter ($\Omega = (\omega a^2/h)\sqrt{\rho/E_2}$) of a simply supported unsymmetric square laminate with a cutout[a]

	Mode I		Modes II and III		Mode IV		Mode V	
d/a	HPE-38	RHPE-18	HPE-38	RHPE-18	HPE-38	RHPE-18	HPE-38	RHPE-18
0.1	97.825	97.836	226.409	226.411	389.617	390.628	423.523	425.531
0.2	88.297	88.312	196.320	195.613	332.090	334.102	367.659	370.212
0.3	91.954	90.518	191.477	193.342	321.165	325.711	365.782	370.113
0.4	100.365	101.502	187.906	197.761	318.027	323.425	369.938	372.260
0.5	115.982	115.991	193.143	190.127	328.436	334.219	392.232	396.314
0.6	143.138	143.782	214.853	216.755	362.860	367.511	455.992	458.732
0.7	192.999	194.010	264.944	267.547	442.918	449.053	621.339	628.420
0.8	299.565	302.611	381.844	383.432	431.993	436.221	632.229	638.011

[a] Ply sequence [±45, 0, 90, ±45]; layer thickness t_p = 0.016 in.; plate slenderness ratio d/t = 104.

Table 5. Modal deflections [±45, 0, 90, ±45] laminate with square cutout

		Deflection at nodes (as shown in Figure 4)							
d/a	Mode[a]	5	7	8	10	11	13	14	16
0.1	SX-SY	0.32	0.66	0.66	0.32	0.32	0.66	0.66	0.32
	SX-AY	0.00	0.37	−0.37	0.21	−0.21	0.37	−0.37	0.0
0.2	SX-SY	0.35	0.7	0.7	0.35	0.35	0.7	0.7	0.35
	SX-AY	0.0	0.4	−0.4	0.23	−0.23	0.4	−0.4	0.0
0.3	SX-SY	0.35	0.68	0.68	0.35	0.35	0.68	0.68	0.35
	SX-AY	0.0	0.48	−0.48	0.26	−0.26	0.48	−0.48	0.0
0.4	SX-SY	0.31	0.65	0.65	0.31	0.31	0.65	0.65	0.31
	SX-AY	0.0	0.71	−0.71	0.33	−0.33	0.71	−0.71	0.0
0.5	SX-SY	0.39	0.67	0.67	0.39	0.39	0.67	0.67	0.39
	SX-AY	0.0	0.72	−0.72	0.29	−0.29	0.72	−0.72	0.0

[a] SX, symmetric about the *X* axis; SY, symmetric about the *Y* axis; AX, antisymmetric about the *X* axis; AY, antisymmetric about the *Y* axis.

mesh is compared to that of RHPE-18, having approximately the same active DOF. Results are included in Table 6. It may be noted that the performance of the original element (HPE-38) in estimating natural frequencies is slightly better than that of the condensed element corresponding to the same (or nearly same) DOF. However, the difference is small, such that the reduced element may be considered more expedient for general dynamic analysis.

CONCLUSION

A reduced, high-precision, triangular element has been developed for the vibration analysis of unsymmetric laminates. A new dynamic condensation procedure is adopted to condense a high-precision 38-DOF element that includes bending-extension coupling. A semianalytical–numerical approach has been used to obtain the element stiffness and

Table 6. Comparison of modal frequencies (rad/s) estimated by HPE-38 and RHPE-18 for a cantilever triangular plate corresponding to similar active DOF

Mode no.	DOF = 60 HPE-38	DOF = 52 RHPE-18	DOF = 104 HPE-38	DOF = 90 RHPE-18	Converged value
1	3.04	3.15	3.01	3.02	2.83
2	12.51	12.82	12.44	12.60	11.84
3	17.85	18.03	17.78	17.85	17.05
4	29.68	30.01	29.52	29.58	29.08

mass matrices in closed form. The reduced high-precision element has only 18 DOF, compared to the 38-DOF original element. Through typical numerical experiments it has been shown that RHPE-18 gives results very close to those with the original element. In view of the elimination of the numerical integration in the element formulation and the reduction of DOF, it is expected that this element will be attractive for the dynamic analysis of unsymmetric laminates.

REFERENCES

1. A. W. Leissa, Advances in Vibration, Buckling and Post Buckling Studies on Composite Plates, *Composite Struct.*, pp. 312–334, 1981.
2. J. N. Reddy, A Review of the Literature on Finite Element Modelling of Laminated Composite Plates, *Shock Vibration Dig.*, vol. 17, pp. 3–8, 1985.
3. R. K. Kapania and S. Raciti, Recent Advances in Analysis of Laminated Beams and Plates, Part ii: Vibrations and Wave Propagation, *AIAA J.*, vol. 27, pp. 935–946, 1989.
4. L. C. Shiau and T. Y. Wu, A High Precision Higher Order Triangular Element for Free Vibration of General Laminated Plates, *J. Sound Vibration*, vol. 161, pp. 265–279, 1993.
5. A. Bhimaraddy, Direct Ply Thickness Computation of Laminated Plates for Which the Kirchhoff's Theory Predicts the Fundamental Frequency within the Specified Degree of Accuracy, *J. Sound Vibration*, vol. 164, pp. 445–458, 1993.
6. G. R. Cowper, E. Kosko, G. M. Lindeberg, and M. D. Olson, A High Precision Triangular Plate Bending Element, Aeronautical Report, LR-514, National Research Council of Canada, December 1968.
7. P. Pederson, On Computer-Aided Analytic Element Analysis and the Similarities of Tetrahedron Elements, *Int. J. Numer. Meth. Eng.*, vol. 11, pp. 611–622, 1977.
8. K. L. Lawrence and R. V. Nambiar, Explicit Expressions for Element Coordinate Transformations by Symbolic Manipulation, *Comput. Struct.*, vol. 32, pp. 277–280, 1989.
9. L. Leff and D. Y. Yun, The Symbolic Finite Element Analysis System, *Comput. Struct.*, vol. 41, pp. 227–231, 1991.
10. D. K. Choi and S. Namura, Application of Symbolic Computation to Two-Dimensional Elasticity, *Comput. Struct.*, vol. 43, pp. 645–649, 1992.
11. L. Meirovitch, Computational Methods in Structural Dynamics
12. M. Pas, Dynamic Condensation, *AIAA J.*, vol. 22, pp. 724–727, 1984.
13. R. D. Henshell and J. H. Ong, Automatic Masters for Eigenvalue Economization, *Earthquake Eng. Struct. Dynam.*, vol. 3, pp. 375–383, 1975.
14. D L. Thomas, Errors in Natural Frequency Calculation Using Eigenvalue Economization, *Int J. Numer. Meth. Eng.*, vol. 18, pp. 1521–1527, 1982.
15. C. Jeyachandrabose and J. Kirkhope, Explicit Formulation for a High Precision Triangular Laminated Anisotropic Thin Plate Finite Element, *Comput. Struct.*, vol. 20, pp. 991–1007, 1985.

16. C. Jeyachandrabose and J. Kirkhope, A High Precision Triangular Laminated Anisotropic Shallow Thin Shell Finite Element, *Comput. Struct.*, vol. 21, pp. 701–723, 1985.
17. O. C. Zienkiewicz, *The Finite Element Method*, 3rd ed. Tata McGraw-Hill, New Delhi, 1979.
18. R. M. Jones, *Mechanics of Composite Materials*, McGraw-Hill, New York, 1975.
19. B. Bhattacharya, A. V. Krishnamurty, and M. S. Bhat, Vibration Analysis of Unsymmetric Laminated Composite Plates Using Condensed High Precision Triangular Elements, Dept. Aerospace Eng., AE-425S, Indian Institute of Science, Bangalore, India, 1995.
20. K. J. Bathe, *Finite Element Procedures in Engineering Analysis*, Prentice-Hall of India, 1990.
21. I. Lee and J. J. Lee, Vibration Analysis of Composite Plate Wing, *Comput. Struct.*, vol. 37, pp. 1077–1085, 1990.
22. H. P. Lee, S. P. Lim, and S. T. Chow, Free Vibration of Composite Rectangular Plates with Rectangular Elements, *Composite Struct.*, vol. 8, pp. 63–81, 1987.
23. A. J. Fricker, A Method for Solving High Order Real Symmetric Eigen Value Problems, *Int. J. Numer. Meth. Eng.*, vol. 19, pp. 1131–1138, 1983.
24. J. N. Reddy and N. D. Phan, Stability and Vibration of Isotropic, Orthotropic and Laminated Plates According to a Higher Order Shear Deformation Theory, *J. Sound Vibration*, vol. 98, pp. 157–170, 1985.
25. R. K. Kapania and P. Mohan, Static, Free Vibration and Thermal Analysis of Composite Plates and Shells Using a Flat Triangular Shell Element, *Comput. Mech.—Int. J.*, vol. 17, pp. 343–357, 1996.